PHYSICAL REVIEW A **69**, 030701(R) (2004)

Collisional properties of trapped cold chromium atoms

Zoran Pavlović,[1] Björn O. Roos,[2] Robin Côté,[1] and H. R. Sadeghpour[3]
[1]*Physics Department, University of Connecticut, 2152 Hillside Road, Storrs, Connecticut 06269-3046, USA*
[2]*Department of Theoretical Chemistry, Chemical Center, P. O. Box 124 S-221 00 Lund, Sweden*
[3]*ITAMP, Harvard-Smithsonian Center for Astrophysics, 60 Garden Street, Cambridge, Massachusetts 02138, USA*
(Received 5 September 2003; revised manuscript received 17 November 2003; published 22 March 2004)

We report on calculations of the elastic cross section and thermalization rate for collision between two maximally spin-polarized chromium atoms in the cold and ultracold regimes, relevant to buffer-gas and magneto-optical cooling. We calculate *ab initio* potential-energy curves for Cr_2 and the van der Waals coefficient C_6, and construct interaction potentials between two colliding Cr atoms. We explore the effect of shape resonances on the elastic cross section, and find that they dramatically affect the thermalization rate. Our calculated value for the *s*-wave scattering length is compared in magnitude with a recent measurement. We propose that a dip in the elastic rate coefficient could be experimentally exploited to obtain an accurate value for the scattering length.

DOI: 10.1103/PhysRevA.69.030701 PACS number(s): 34.50.−s, 34.20.−b, 31.15.Ne

Collisions of atoms at ultracold temperatures have received considerable attention because of their importance in cooling and trapping of atoms [1], their role in high-precision spectroscopy [2], and the realization of Bose-Einstein condensation (BEC) [3]. Recent experiments with chromium [4–7] emphasize the need for theoretical studies of its scattering properties. The interest in cooling Cr stems from its particular properties; in its ground state $^7S_3$, it possesses a large magnetic moment, $6\mu_B$ (μ_B is the Bohr magneton), making it an ideal atom for buffer cooling in a purely magnetic trap [7], as well as for magneto-optical trapping (MOT) [4]. In addition, anisotropic long-range interactions, such as chromium's magnetic dipole-dipole interactions [8], may lead to novel phenomena in BECs [9,10]. The existence of a stable fermionic isotope, ^{53}Cr, opens the possibility of obtaining fermionic degenerate gas using sympathetic cooling. A not so-desirable byproduct of large-spin collision is the important "bad" scattering that depletes the trap.

On the theoretical front, the electronic spectrum of the Cr_2 dimer poses considerable challenge. Chromium is the first atom in the periodic table with a half-filled *d* shell [the ground electronic configuration is Cr($3d^5 4s, ^7S_3$)] and the Cr_2 dimer is one of the most extreme cases of multiple metal-metal bonding. To date, the best attempt to calculate its interaction potential curves is a multiconfiguration second-order perturbation theory with complete active space self-consistent field (CASSCF/CASPT2) [11,12]. While spectroscopic constants for the ground electronic state ($^1\Sigma_g^+$ symmetry) exist [13], there is no spectroscopic data available when two Cr atoms interact in the $^{13}\Sigma_g^+$ molecular symmetry.

In this Rapid Communication, we explore the collisional properties of Cr atoms at cold and ultracold temperatures by revisiting the electronic structure of the dimer. More accurate Born-Oppenheimer potential-energy curves dissociating to two ground state Cr atoms are calculated. The van der Waals interaction coefficient C_6, obtained semiempirically from available bound atomic transition matrix elements and photoionization cross sections, was found to be 745 ± 55 a.u., where 1 a.u. $= 9.57 \times 10^{-80}$ J m^6. Elastic cross sections and collision rate coefficients are calculated using the newly constructed potential curves and compared against two recent measurements [5,7]. We also investigated the bound and resonance structure in the $^{13}\Sigma_g^+$ state as a function of rotational angular momenta.

The potential curves for Cr_2, shown in Fig. 1, were constructed from three regions joined smoothly together. First, *ab initio* potential curves were computed using the CASSCF/CASPT2 method [11,12]. The CASSCF wave function is formed by distributing 12 electrons in the 3*d* and 4*s* active orbitals while keeping the inactive 1*s*, 2*s*, 2*p*, 3*s*, and 3*p* orbitals occupied. The remaining dynamical electron correlation energy is obtained through second-order perturbation theory (CASPT2). The basis set used in the calculations is of the atomic natural orbital (ANO-RCC) type contracted to $9s8p7d5f3g$. This basis set is relativistic and includes functions for correlating the 3*s* and 3*p* electrons [14]. The

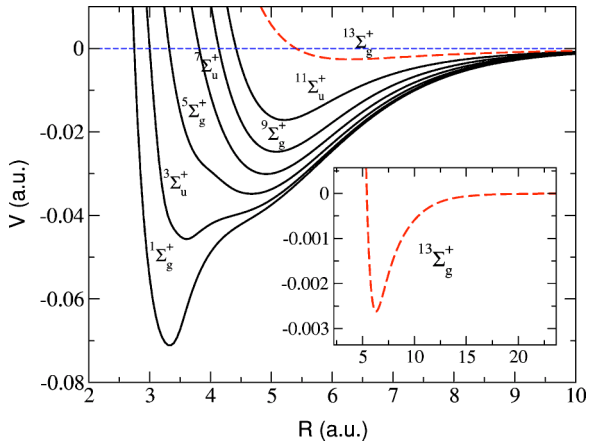

FIG. 1. (Color online) Potential curves for the ground-state manifold of Cr_2 computed with the CASSCF/CASPT2 method. The maximally spin-stretched electronic state $^{13}\Sigma_g^+$ is shown as a dashed line and in detail in the inset.

Douglas-Kroll Hamiltonian was used with Fock-type correction $0.5\mathbf{g}_1$, see Ref. [15]. The full counterpoise method was used to correct energies for the basis set superposition error. Convergence to 10^{-10}, in hartrees, was achieved, and numerical accuracy in computed binding energies is about 10^{-8}.

For separations $R \leqslant R_1^\lambda$, where R_1^λ is the smallest separation of the *ab initio* data for the potential energy $V_\lambda(R)$, each curve was joined smoothly to the exponential form $V_\lambda(R) = c_\lambda \exp(-b_\lambda R)$, with the coefficients c_λ and b_λ determined by matching both the potential curve and its first derivative continuously at R_1^λ. At large values of R, the *ab initio* data were matched to the asymptotic form $V_\lambda(R) = -C_6/R^6 + A_\lambda R^\nu e^{-\beta R}$, where the parameters of the exchange energy are determined according to Smirnov and Chibisov [16]: $\nu = (7/\beta) - 1$ and $\beta = 2\sqrt{2I}$, where I is the ionization energy of the atom ($I = 0.248\,664\,314$ a.u. for Cr). The parameters A_λ were found by fitting the *ab initio* curves at separations where the exchange energy was still considerable (e.g., R between 10 and 14 a.u. for $^{13}\Sigma_g^+$).

The C_6 coefficient was calculated using

$$C_6 = \frac{3}{2}\left(\frac{e^2\hbar^2}{m}\right)^2 \frac{1}{|E_0|^3}\left\{\sum_{i,j}\frac{f_{0i}f_{0j}}{v_i v_j (v_i + v_j)} + 2\sum_i \frac{f_{0i} G(1+v_i)}{v_i} + \int_0^\infty \frac{(df/d\epsilon) G(2+\epsilon) d\epsilon}{(1+\epsilon)}\right\}, \tag{1}$$

where contributions of bound-bound, bound-free, and free-free transitions are given by the first, second, and third term, respectively. This expression is derived from London's formula [17], assuming $v_i = 1 - E_i/E_0$ and $\epsilon = -E/E_0$, where E_0, E_i, and E are the ground, ith excited state, and continuum energies, respectively, f_{0i} are the oscillator strengths pertaining to transitions to the ground state, and df/dE accounts for the continuum spectrum. The auxiliary function $G(z)$ is given by

$$G(z) = \int_0^\infty \frac{(df/d\epsilon) d\epsilon}{(1+\epsilon)(z+\epsilon)}. \tag{2}$$

Values of the oscillator strengths and energy levels for discrete transitions were taken from the NIST Atomic Spectra Database [18] and Ref. [19]. The continuum oscillator strength $df/d\epsilon$ was found using Verner's [20] analytic fits for partial photoionization cross sections and autoionization measurements in the range of $3p$-nd "giant" resonances [21]. If we measure dE in atomic units, then

$$\frac{df}{dE} = \frac{1}{2\pi^2 \alpha a_0^2}\sigma_{\rm ph}, \tag{3}$$

where α is the fine-structure constant, a_0 is the Bohr radius, and $\sigma_{\rm ph}$ is the photoionization cross section. The dimensionless $df/d\epsilon$ is obtained by multiplying Eq. (3) by $|E_0|$ (also in a.u.).

We assess the quality of the semiempirical computation of the van der Waals coefficient by satisfying two sum rules, namely, the zeroth and the inverse second moments, i.e., $S(0) = N$ and $S(-2) = \alpha_0$, where N is the number of electrons (24 for Cr) and α_0 is the static polarizability. We obtained $\Sigma_i f_{0i} = 22.3$ and $\alpha_0 = 85.0$ a.u., in agreement with a recommended value $82 \pm 20\%$ a.u. [22]. The resulting dispersion coefficient is expected to have an accuracy of about 7%, $C_6 = 745 \pm 55$ a.u.

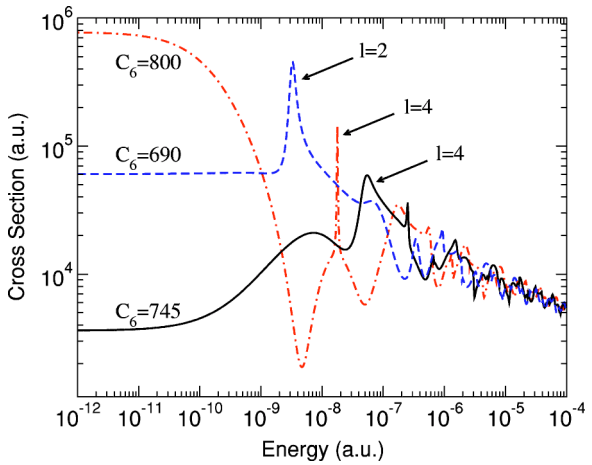

FIG. 2. (Color online) Elastic cross sections for collision between two bosonic Cr atoms as a function of energy. The three curves are labeled by the value of the C_6 coefficient used to construct the interaction potential in each case. See text for details.

Specifically, we find that the discrete (continuum) contributions to the oscillator strength and polarizability are 1.92(20.38) and 78.7(6.3) a.u., respectively. The discrete-discrete, discrete-continuum, and continuum-continuum contributions to the dispersion terms in Eq. (1), are 568, 155.4, and 21.8, respectively, all in a.u., the $3p$-nd resonances contribute 16.7 a.u. to C_6. The existence of large amplitude, optically accessible $3p$-nd autoionizing resonances in Cr has been the subject of considerable attention over the last decade due to its uniqueness to chromium [21].

The elastic cross section for the collision of two ^{52}Cr atoms, composite bosons, in the $^{13}\Sigma_g^+$ potential, expanded over the rotational quantum number l, is

$$\sigma_{\rm el}(E) = \frac{8\pi}{k^2}\sum_{l\ \rm even}(2l+1)\sin^2\delta_l, \tag{4}$$

where $E = \hbar^2 k^2/2\mu$ is the kinetic energy of relative motion, μ is the reduced mass, and $\delta_l(k)$ is the lth scattering phase shift in the electronic state $^{13}\Sigma_g^+$. In the low-energy limit, the elastic cross section behaves as

$$\sigma_{\rm el}(E) \overset{E\to 0}{\to} \frac{8\pi a^2}{k^2 a^2 + \left(1 - \frac{1}{2} r_e a k^2\right)^2}, \tag{5}$$

where scattering length a is determined at the zero-energy s-wave limit, $a = -\lim_{k\to 0}(1/k)\tan\delta_0(k)$, while the effective range r_e can be found by fitting the cross section, from an integral expression [23], or using quantum defect theory [24].

TABLE I. Calculated scattering length and effective range for different models of the $^{13}\Sigma_g^+$ interaction potentials, in a.u.

C_6	a	r_e
690	49	98
745	12	2600
800	−176	213

The cross section as a function of the collision energy is shown in Fig. 2 for three different $^{13}\Sigma_g^+$ interaction potentials, each constructed by matching at large distances to the upper, lower, and mean values of C_6 within the uncertainty in our calculation of this quantity. At collision energies larger than $E \sim 10^{-6}$ a.u., aside from the shape resonance structure, the cross sections differ little in magnitude, but are dramatically dissimilar in the *s*-wave limit. From an analysis of a recent MOT measurement of elastic rate coefficient [5] and the robustness of the cross section to uncertainties in the models for the interaction potential at energies $E \gtrsim 10^{-6}$ a.u. (see discussion of rate coefficients below), we find our results to be consistent with $C_6 = 800$ a.u.; hence the most likely value for the scattering length for the $^{13}\Sigma_g^+$ state is large and negative (see Table I), indicating that evaporative cooling should be efficient. In Ref. [5], the magnitude of the scattering length is extracted from a fit to the experimental collision rate coefficient, which agrees with our most probable value, but the authors [5] conclude that the sign is most likely positive, with which our results disagree. Our calculated effective range expansion coefficients agree closely with the results obtained using the quantum-defect method of Gao [24]. That our calculated scattering length varies from moderate positive values to relatively large negative values is indicative of a zero crossing, and not the formation of an extra bound state (an additional level appears for $C_6 \sim 815$ a.u., outside our range of values). As the collision energy increases, the appearance of shape resonances can lead to large cross sections. Although the details of the resonance structure, i.e., profile and energy position, depend on the details of the potentials, their exact effect on the elastic rate coefficient is averaged out at temperatures for which the shape resonances matter. This is portrayed in Fig. 3, where the rate coefficients for the three different potentials are similar for temperatures higher than 100 mK.

Our calculated rate coefficients are larger than those measured in Ref. [7] by more than an order of magnitude. We do not yet understand the origin of this discrepancy—an attempt at modifying the potential in the long range and in the short range resulted in practically similar results. The shape and magnitude of the calculated rate coefficient for $C_6 = 800$ a.u. agrees in both magnitude and shape with the MOT experimental results, see Fig. 3 of Ref. [5]. The decline in the rate coefficient for $T > 100$ μK, as seen in our calculation, followed by a rise for $T > 1$ mK, is due to the appearance of the $l = 4$ shape resonance in Fig. 2. The experimental determination of the dip in the elastic rate coefficient could potentially be used to infer a more accurate value of C_6 and hence the scattering length. Although our neglect of the contributions from higher-order dispersion terms, C_8, and C_{10}, etc., should not affect the cross section at millikelvin temperatures, their influence at microkelvin temperatures ought to be investigated. An experimental determination of the dip in the elastic rate coefficient should help in this regard.

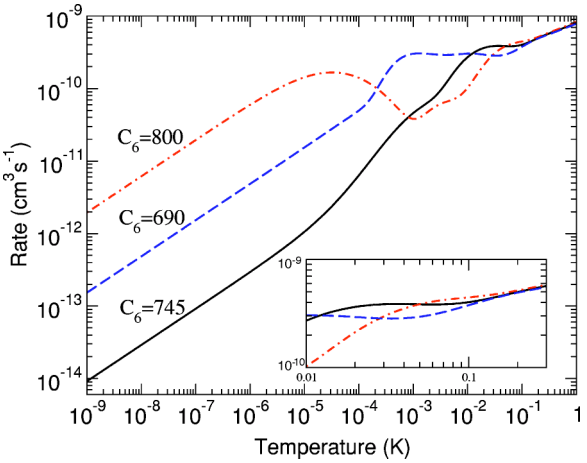

FIG. 3. (Color online) The calculated collision rate coefficient as a function of temperature. At temperatures above 100 mK, the different calculated rates are practically the same. The plateau region is shown in the inset. The dip and the subsequent rise in the rate coefficient (for $C_6 = 800$ a.u.) near $T \sim 10^{-4} - 10^{-1}$ K are due to the appearance of the $l = 4$ shape resonance.

In Fig. 4, we give the bound and shape resonance structure in the $^{13}\Sigma_g^+$ potential-energy curve with $C_6 = 745$ a.u., as a function of the rotational angular momentum l. Due to symmetry, only even values of l appear in the collision between two maximally polarized Cr atoms. The grouping of the levels in solid and dashed lines indicates the disappearance of a bound level and the appearance of an additional shape resonance.

A plateau in the observed elastic collision rate coefficient in the range 10 mK $< T <$ 300 mK exists [7,8] and is reproduced in our calculation in Fig. 3. It appears that this plateau

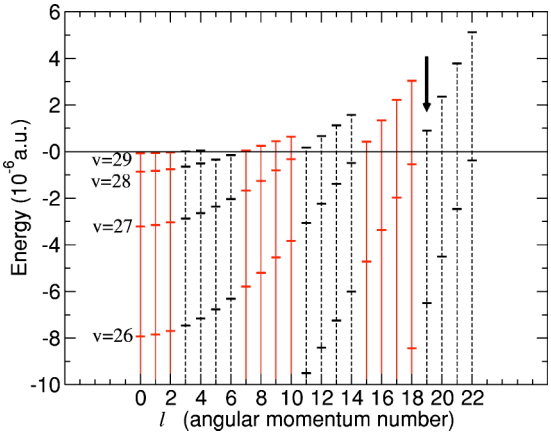

FIG. 4. (Color online) The bound and shape resonance structure in the Cr_2 $^{13}\Sigma_g^+$ potential energy curve (for $C_6 = 745$ a.u. as a function of l. The narrowest resonance is indicated with the arrow, whose lifetime is more than two seconds.

is produced by the confluence of many collisionally excited shape resonances in this temperature range.

We have calculated *ab initio* interaction potentials for collision of two Cr atoms, and obtained the long-range van der Waals coefficient. Elastic collision cross section and rate coefficient for two maximally spin-polarized chromium atoms have been computed in the cold and ultracold regimes and compared with available experimental data. The effect of partial-wave shape resonances is studied, and the most probable values for the *s*-wave scattering length and effective range have been obtained from a comparison with a recent MOT experiment $a=-176$ a.u. and $r_e=213$ a.u. The disagreement with the buffer-gas cooling rate coefficient results is not fully understood and the inelastic loss rate, expected to be due to spin dipole interaction, is under investigation. Additional spectroscopic and collision measurements will help us to calibrate the interaction potentials and pin down an accurate value for the scattering length.

The work of Z.P. and R.C. was supported in part by the National Science Foundation Grant No. PHY0140290 and the University of Connecticut Research Foundation. The authors would like to thank J. Doyle and R. Krems for fruitful discussions. This work was supported by the National Science Foundation through a grant for the Institute for Theoretical Atomic Molecular and Optical Physics at Harvard University and Smithsonian Astrophysical Observatory. H.R.S. is grateful to K. Andersson for access to numerical data for an earlier calculation of the potential curves and to P. O. Schmidt and R. deCarvalho for valuable correspondence. B.O.R. thanks the Swedish Science Research Council (VR) for financial support.

[1] S. Chu, Rev. Mod. Phys. **70**, 685 (1998); C. N. Cohen-Tannoudji, *ibid.* **70**, 707 (1998); W. C. Phillips, *ibid.* **70**, 721 (1998).

[2] J. Weiner, V. S. Bagnato, S. C. Zilio, and P. S. Julienne, Rev. Mod. Phys. **71**, 1 (1999).

[3] See A. J. Leggett, Rev. Mod. Phys. **73**, 307 (2001), and references therein.

[4] C. C. Bradley *et al.*, Phys. Rev. A **61**, 053407 (2000).

[5] P. O. Schmidt *et al.*, Phys. Rev. Lett. **91**, 193201 (2003).

[6] Stuhler J. *et al.*, Phys. Rev. A **64**, 031405 (2001); S. Giovanazzi, A. Görlitz, and T. Pfau Phys. Rev. Lett. **89**, 130401 (2002).

[7] J. M. Doyle *et al.*, Phys. Rev. A **65**, 021604 (2002); J. D. Weinstein *et al.*, *ibid.* **57**, R3173 (1998).

[8] Robert deCarvalho (private communication).

[9] L. Santos, G. V. Shlyapnikov, P. Zoller, and M. Lewenstein, Phys. Rev. Lett. **85**, 1791 (2000).

[10] M. Baranov *et al.*, Phys. Scr., T **T102**, 74 (2002).

[11] B. O. Roos, in *Advances in Chemical Physics, Ab Initio Methods in Quantum Chemistry*, edited by K. P. Lawley (Wiley, Chichester, 1987); B. O. Roos *et al.*, in *Advances in Chemical Physics; New Methods in Computational Quantum Mechanics*, edited by I. Prigogine and S. A. Rice (Wiley, New-York, 1996).

[12] B. O. Roos, and K. Andersson, Chem. Phys. Lett. **245**, 215 (1995); B. O. Roos, Collect. Czech. Chem. Commun. **68**, 265 (2003); K. Andersson, Chem. Phys. Lett. **237**, 212 (1995).

[13] S. M. Casey, and D. G. Leopold, J. Phys. Chem. **97**, 816 (1993); V. E. Bondybey and J. H. English, Chem. Phys. Lett. **94**, 443 (1983).

[14] The primitive basis set was 21*s*15*p*10*d*6*f*4*g*. These basis sets are under construction for the entire periodic system [B. O. Roos (unpublished)].

[15] K. Andersson, Theor. Chim. Acta **91**, 31 (1995).

[16] B. M. Smirnov and M. I. Chibisov, Sov. Phys. JETP **21**, 624 (1965); E. L. Duman and B. M. Smirnov, Opt. Spectrosc. **29**, 229 (1970).

[17] H. Margenau, Phys. Rev. **56**, 1000 (1939).

[18] NIST Atomic Spectra Database: http://physics.nist.gov/cgi-bin/AtData/main_asd

[19] D. A. Verner, P. D. Barthel, and D. Tytler, Astron. Astrophys., Suppl. Ser. **108**, 287 (1994).

[20] D. A. Verner, and D. G. Yakovlev, Astron. Astrophys., Suppl. Ser. **109**, 125 (1995).

[21] Th. Dohrmann *et al.*, J. Phys. B **29**, 4641 (1996); V. K. Dolmatov, *ibid.* **26**, L393 (1993).

[22] *CRC Handbook of Chemistry and Physics*, 83rd ed. Secs. 10–163 (CRC Press, Boca Raton, 2002), LLC, www.crcpress.com

[23] N. F. Mott, and H. S. W. Massey, *The Theory of Atomic Collisions*, 3rd ed. (Clarendon Press, Oxford, 1965).

[24] B. Gao, Phys. Rev. A **58**, 4222 (1998).